0026-895X/06/7002-549–561$20.00
MOLECULAR PHARMACOLOGY
Copyright © 2006 The American Society for Pharmacology and Experimental Therapeutics
Mol Pharmacol 70:549–561, 2006

Vol. 70, No. 2
25304/3130047
Printed in U.S.A.

Aryl Hydrocarbon Receptor Activation Produces Heart-Specific Transcriptional and Toxic Responses in Developing Zebrafish[S]

Sara A. Carney, Jing Chen, C. Geoffrey Burns, Kong M. Xiong, Richard E. Peterson, and Warren Heideman

Molecular and Environmental Toxicology Program (S.A.C., R.E.P., W.H.), Pharmaceutical Sciences (J.C., R.E.P., W.H.), and Biomolecular Chemistry (K.M.X., W.H.), University of Wisconsin, Madison, Wisconsin; and Cardiovascular Research Center, Massachusetts General Hospital, Harvard University, Charlestown, Massachusetts (C.G.B.)

Received April 5, 2006; accepted May 19, 2006

ABSTRACT

Proper regulation of the aryl hydrocarbon receptor (AHR), a ligand-activated transcription factor, is required for normal vertebrate cardiovascular development. AHR hyperactivation by 2,3,7,8-tetrachlorodibenzo-*p*-dioxin (TCDD) during zebrafish (*Danio rerio*) development results in altered heart morphology and function, culminating in death. To identify genes that may cause cardiac toxicity, we analyzed the transcriptional response to TCDD in zebrafish hearts. Zebrafish larvae were exposed to TCDD for 1 h at 72 h after fertilization (hpf), and the hearts were extracted for microarray analysis at 1, 2, 4, and 12 h after exposure (73, 74, 76, and 84 h postfertilization). The remaining body tissue was also collected at each time for comparison. TCDD rapidly induced expression in 42 genes within 1 to 2 h of exposure. These genes function in xenobiotic metabolism, proliferation, heart contractility, and pathways that regulate heart development. Furthermore, these expression changes preceded signs of cardiovascular toxicity, characterized by decreased stroke volume, peripheral blood flow, and a halt in heart growth. This identifies strong candidates for important AHR target genes. It is noteworthy that the TCDD-induced transcriptional response in the hearts of zebrafish larvae was substantially different from that induced in the rest of the body tissues. One of the biggest differences included a cluster of genes that were down-regulated 12 h after exposure in heart tissue, but not in the body samples. More than 70% of the transcripts in this heart-specific cluster promote cellular growth and proliferation. Thus, the developing heart stands out as being responsive to TCDD at both the level of toxicity and gene expression.

The aryl hydrocarbon receptor (AHR) mediates responses to toxic polycyclic aromatic hydrocarbons found in the environment. The pathway is activated by specific hydrocarbon ligands that bind to cytoplasmic AHR. Activated AHR translocates to the nucleus and dimerizes with the aryl hydrocarbon receptor nuclear translocator (ARNT). The AHR/ARNT heterodimer binds to xenobiotic response elements to regulate transcription of target genes (Schmidt and Bradfield, 1996; Rowlands and Gustafsson, 1997). The most thoroughly understood AHR target genes encode enzymes that eliminate toxic compounds encountered in the environment. AHR-mediated induction of these enzymes forms a homeostatic loop for eliminating toxic compounds.

In addition to this adaptive response, it is now believed that the AHR/ARNT complex also plays a physiological function during development (Hahn, 2003). Manipulation of AHR activity disrupts the normal development of specific organs at specific developmental stages. This is very apparent in cardiovascular development: both overactivation and underactivation of the AHR/ARNT pathway during early life stages can disrupt vertebrate cardiovascular development.

Ahr-null mice show vascular defects (Fernandez-Salguero et al., 1996; Schmidt et al., 1996; Lahvis et al., 2000; Walisser et al., 2004) as well as defects in heart development (Fernan-

This work was supported by the University of Wisconsin Sea Grant Institute, National See Grant College Program, National Oceanic and Atmospheric Administration, U.S. Department of Commerce grant number NA16RG2257, Sea Grant Project Numbers R/BT-16 and R/BT-17, and by National Institutes of Health grant R01-ES012716 from the National Institute of Environmental Health Sciences (to W.H. and R.E.P.). This work was also supported by National Institutes of Health grant T32-ES07015 from the National Institute of Environmental Health Sciences (to S.A.C.) and the Molecular and Environmental Toxicology Program (University of Wisconsin-Madison) National Institute of Environmental Health Sciences Training grant contribution 357.

Article, publication date, and citation information can be found at http://molpharm.aspetjournals.org.

doi:10.1124/mol.106.025304.

[S] The online version of this article (available at http://molpharm.aspetjournals.org) contains supplemental material.

ABBREVIATIONS: AHR, aryl hydrocarbon receptor; ARNT, aryl hydrocarbon receptor nuclear translocator; TCDD, 2,3,7,8-tetrachlorodibenzo-*p*-dioxin; hpf, hours postfertilization; DMSO, dimethyl sulfoxide; PCR, polymerase chain reaction; EDV, end-diastolic volume; ESV, end-systolic volume; EF, ejection fraction; SV, stroke volume; CO, Cardiac output; HR, heart rate.

dez-Salguero et al., 1997; Thackaberry et al., 2002; Lund et al., 2003), whereas AHR activation in mice exposed to the AHR agonist 2,3,7,8-tetrachlorodibenzo-*p*-dioxin (TCDD) during gestation produces alterations in heart size, myocyte proliferation, and basal and isoproterenol-responsive heart rate. An initial reduction in heart weight in developing mice seems to cause progressive cardiac hypertrophy (Lin et al., 2001; Thackaberry et al., 2005b). TCDD exposure during development also causes alterations in heart structure and function in birds (Cheung et al., 1981; Rifkind et al., 1985; Brunstrom and Lund, 1988; Canga et al., 1988, 1993; Walker et al., 1997; Walker and Catron, 2000; Sommer et al., 2005), including a reduction in cardiac myocyte number, a decrease in myocyte proliferation, and an increase in apoptosis (Ivnitski et al., 2001).

In embryonic fish, TCDD at parts-per-billion concentrations results in marked heart malformations, reduced peripheral blood flow, pericardial edema, and hemorrhage (Helder, 1980, 1981; Wisk and Cooper, 1990; Spitsbergen et al., 1991; Henry et al., 1997; Elonen et al., 1998; Hornung et al., 1999; Guiney et al., 2000; Teraoka et al., 2002). TCDD reduces heart size during development in both zebrafish and trout (Hornung et al., 1999; Antkiewicz et al., 2005). In zebrafish embryos, a reduction in cardiomyocyte numbers is the earliest known response to TCDD and is associated with compaction of the ventricle, elongation of the heart, and increased incidence of ventricular standstill. Effects on the heart can be seen before any observable effect on blood flow (Antkiewicz et al., 2005).

These developmentally specific responses suggest that the toxic responses are due to misregulation of a signaling pathway that is important for normal development. This is strengthened by recent work in which developmental defects in hypomorphic *Ahr* and *Arnt* mutant mice were reversed by using TCDD to titrate AHR activity toward normal levels (Walisser et al., 2004). In addition, there is growing evidence that the adaptive detoxification response, involving genes such as *cyp1a,* does not play a major role in the prominent developmental defects produced by TCDD (Carney et al., 2004). If TCDD produces cardiac toxicity through the misregulation of target genes normally controlled by the AHR/ARNT pathway (Bunger et al., 2003; Walisser et al., 2004) then identification of AHR/ARNT target genes should provide important insights into both TCDD toxicity and normal heart development.

Microarrays have been used to identify global gene expression changes induced by TCDD in a variety of vertebrate cell types (Puga et al., 2000b; Frueh et al., 2001; Martinez et al., 2002; Fisher et al., 2004; Jin et al., 2004; Vezina et al., 2004; Hanlon et al., 2005). A recent study identified TCDD-induced gene expression changes in whole zebrafish embryos after a 3-day exposure to TCDD, a point at which cardiac toxicity is strongly manifested (Handley-Goldstone et al., 2005). The study found TCDD-induced changes consistent with late stage heart failure, including transcripts involved in sarcomere structure and mitochondrial energy transfer. Whereas these gene expression changes are clearly associated with the pathological changes in the heart, the relationship between the transcript changes seen 3 days after initial exposure and the direct targets of AHR/ARNT is difficult to assess. In addition, important changes in transcripts in the heart might easily be masked by the signal from mRNA produced in the rest of the body, which is far more massive than the heart.

To identify AHR/ARNT target genes in the heart, we exposed zebrafish embryos to TCDD beginning at 72 h after fertilization (hpf) and measured TCDD-induced gene expression changes in the hearts of zebrafish larvae at 1, 2, 4, and 12 h after exposure, correlating the gene expression changes with the emergence of toxic responses. Because the hearts of zebrafish larvae are less than 200 μm in diameter and weigh less than 100 μg (Hu et al., 2000; Antkiewicz et al., 2005), we used a novel dissection method to rapidly extract sufficient numbers of hearts for Affymetrix microarray hybridization (Burns and MacRae, 2006). TCDD induced expression of a group of genes within only 1 to 2 h of exposure, identifying potential candidate AHR/ARNT targets. Toxic responses were not observed until 8 h after exposure. At 12 h after exposure, we observed repression of a considerably larger group of genes. More than 70% of these transcripts are involved in cell growth. This coincided with a halt in cardiomyocyte growth. It is remarkable that most of the alterations in expression were heart-specific: at all time points, the transcriptional response to TCDD in hearts was far more substantial than the response in the extracardiac tissues.

Materials and Methods

Zebrafish Embryos. Fertilized *cmcl2*::*GFP*+/− zebrafish (*Danio rerio*) embryos were obtained from adult male *cmcl2*::*GFP*+/+ (AB background) fish bred with female AB fish, maintained at 27° with a 14-h/10-h light/dark cycle, and used for each experiment except those experiments carried out to assess heart looping and myocyte cell number. To assess heart looping without pigment blocking, albino embryos were used (AB background). To assess myocyte cell number, *cmcl2*::*dsRed2-nuc*+/+ embryos were used (AB background). All embryos were raised in egg water (60 μg/ml Instant Ocean Salts; Aquarium Systems, Mentor, OH).

Waterborne Exposure of Larvae to TCDD. Recently hatched larvae were statically exposed to 2,3,7,8-tetrachlorodibenzo-*p*-dioxin (TCDD, > 99% purity; Chemsyn, Lenexa, KS) for 1 h from 72 to 73 hpf by maintaining larvae in egg water containing either vehicle [0.1% dimethyl sulfoxide (DMSO)] or TCDD (1 ng/ml) as described previously (Carney et al., 2004).

Experimental Design. For experiments assessing cardiovascular toxicity n was defined as the set of larvae exposed to waterborne TCDD or vehicle in a single vial. For microarray analysis of gene expression changes in the heart three replicates ($n = 3$) were collected for each treatment at each time point. Each replicate consisted of 500 hearts pooled from six blocks. For each block, 130 larvae were exposed to either TCDD or vehicle in a single vial before the heart extraction procedure, which yielded approximately 80 to 90 hearts/130 larvae. For microarray analysis of gene expression changes in the body, 20 larval bodies were collected after the heart extraction procedure at 73, 74, 76, and 84 hpf from larvae exposed to TCDD or vehicle in a single vial at 72 hpf for 1 h. Three replicates ($n = 3$) were collected for each treatment at each time point. For real-time PCR analysis of gene expression changes in three heart replicates ($n = 3$) were collected in the same manner as for the microarray analysis. The sample collection times are shown in Fig. 1.

Heart Extraction. Hearts were extracted from larvae by shear forces applied by passing them through a needle and syringe (Burns and MacRae, 2006). Larvae were gently anesthetized with Tricaine-S (Aquatic EcoSystems, Apopka, FL), placed in a microcentrifuge tube with Lebovitz's L15 media + 10% fetal bovine serum (Invitrogen, Carlsbad, CA), and mounted on a ring stand. A 5-cc syringe with a 19-gauge needle was mounted so the tip the needle was near the

bottom of the microcentrifuge tube. The syringe plunger was pulled up and pushed down at constant rate of one push or pull per second for 1-min. The sheared larvae were removed from the microcentrifuge tube and dripped over a 105-μm mesh filter, which retained the bodies and allowed the hearts to pass through. The filtrate containing the hearts was then dripped over a 40-μm mesh filter that retained the hearts and permitted smaller debris tissue to pass through. The hearts, expressing green fluorescent protein, were rinsed from the 40-μm mesh filter into a 60-mm Petri dish with fresh media (Lebovitz's L15 media + 10% fetal bovine serum), then located with epifluorescence and immediately collected into a clean microcentrifuge tube on ice. Samples were centrifuged at 3000*g* for 5 min to pellet the hearts. The supernatant was removed, and the pelleted hearts were snap frozen in liquid nitrogen and stored at −80°C.

Microarray Analysis. Total RNA was isolated from 500 extracted hearts for each treatment group using a QIAGEN RNeasy Mini kit according to the manufacturer's protocol (QIAGEN, Valencia, CA). cDNA and biotin-labeled cRNA were produced from 1 μg of each RNA sample using the Affymetrix One-Cycle Target Labeling and Control Reagents kit according to the manufacturer's protocol (Affymetrix, Santa Clara, CA). Samples were hybridized on Affymetrix GeneChip Zebrafish Arrays following the procedure in the Affymetrix *GeneChip Expression Analysis Technical Manual*. In brief, 15 μg of fragmented biotin-labeled cRNA was hybridized to a zebrafish array for 16 h at 45° with rotation. After hybridization, arrays were washed and stained with streptavidin-phycoerythrin on an Affymetrix Fluidics Station 400 using protocol EukGE-W32v4. Arrays were scanned using the Agilent Gene Array Scanner. The relative abundance of each transcript was calculated by Affymetrix Microarray Suite (MAS) 5.0 software. Intensity values within each replicate for each treatment and time point were averaged for each transcript represented on the array. To determine the change in gene expression induced by TCDD, the $\log_2$(TCDD/DMSO) was calculated from the averaged intensity values for each transcript represented on the array. Significant changes were determined by two-class unpaired Significance Analysis of Microarray (SAM) with a ≤10% false discovery rate for each time point using TIGR MultiExperiment Viewer (TMEV) software (Saeed et al., 2003) from The Institute for Genomic Research (TIGR). Subsequent hierarchical cluster analysis [average linkage cluster of genes, Euclidean distance (Eisen et al., 1998)] with TMEV software was performed on significant gene expression changes of 2-fold or more to group genes with similar TCDD-induced expression patterns. Raw microarray data were deposited in the European Bioinformatics Institute (EMBL-EBI) ArrayExpress database (accession number E-MEXP-758). TCDD-induced expression changes for genes selected from each cluster were confirmed with quantitative real-time PCR. Genes not annotated by Affymetrix MAS 5.0 software were blasted against the zebrafish genome (assembly version 37, February 2006) through the Ensembl Zebrafish Genome Browser maintained by the Wellcome Trust Sanger Institute. Protein translations of transcripts that mapped to known or novel zebrafish genes were blasted against the UniProt knowledgebase (Swiss-Prot + TrEMBL) through the ExPASy Proteomics Server maintained by the Swiss Institute of Bioinformatics. Gene functions were assigned based on results of peer-reviewed published primary literature.

Real-Time PCR. Total RNA was isolated from three replicates of 500 extracted hearts for each treatment group ($n = 3$ for TCDD and DMSO treatments at 73, 74, 76, and 84 hpf) using a QIAGEN RNeasy Mini kit according to the manufacture's protocol. cDNA was produced from 1 μg of each RNA sample using SuperScript II (Invitrogen) and anchored oligo(dT) primer (Integrated DNA Technologies, Coralville, IA). Quantitative real-time PCR using specific gene primers was performed using the Light Cycler (Roche Applied Science, Indianapolis, IN), with 1 μl of each cDNA sample in the presence of SYBR Green according to the manufacture's instructions. Gel electrophoresis and thermal denaturation (melt curve analysis) were used to confirm specific product formation. mRNA levels of analyzed genes were normalized to β-actin mRNA to generate a relative expression ratio. The TCDD-induced change in mRNA expression is reported as the $\log_2$ (TCDD relative expression ratio/DMSO relative expression ratio). Only significant TCDD-induced changes ($p \leq 0.05$) are reported. All oligonucleotide primers were synthesized by Integrated DNA Technologies (Coralville, IA) and are written 5′ to 3′. Oligonucleotides for real-time PCR were: β-actin: forward, aagcaggagtacgatgagtc; reverse, tggagtcctcagatgcattg; cyp1a: forward, tgccgatttcatccctttcc; reverse, agagccgtgctgatagtgtc; mcm2: forward, aaagacgttcgcacggtatc; reverse, aagtccgggagactccagat; atp1α3b: forward, gcaactcagtgttccagcag; reverse, gaggatgttggggacttgag; endothelin1: forward, gctggaatacctcgctcaag; reverse, gcacatggctttggctttat, hey2: forward, cacccaacagcagctttaga; reverse, cccccaaacaaacagtagtga; pcna: forward, ctctgtccaagacggtcaca; reverse, acaatcgggaatccattgaa; irx4a: forward, gttatcgcgggaagttgtgt; reverse, caaggtccgagtccgtctaa; myogenin: forward, gccttggagggcttaatttc; reverse, gaatcagccttcctgactgc; and pik3r3: forward, tggtagcgaagtggtctgtc; reverse, aggcagccacaatgaaaagt.

Red Blood Cell Perfusion Rate. Red blood cell perfusion rate was measured in an intersegmental vessel of the trunk as an index

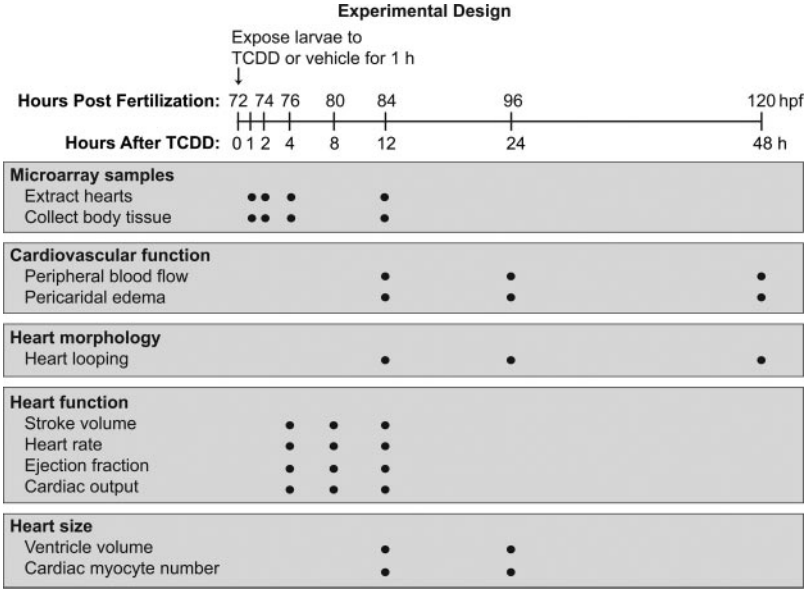

Fig. 1. Schematic of experimental design illustrating the timing of microarray analysis and assessment of cardiac function and heart morphology in zebrafish larvae exposed to TCDD at 72 hpf.

of regional blood flow as described previously (Teraoka et al., 2002; Prasch et al., 2003; Carney et al., 2004). In brief, the number of red bloods cells passing a defined point in the intersegmental vessel in 10 s was counted from time-lapse videomicroscopy recordings.

Pericardial Sac Area. The magnitude and incidence of TCDD-induced pericardial edema in larvae was determined by quantitation of the pericardial sac area as described previously (Prasch et al., 2003; Carney et al., 2004). In brief, the pericardial sac area was outlined in lateral view images and quantitated using Scion Image for Windows (Scion Corporation, Frederick, MD).

Heart Looping. To assess the angle of looping between the atrium and ventricle, time-lapse recordings of the beating heart were made from larvae mounted in 3% methylcellulose and carefully positioned for time-lapse imaging of the ventral view of the heart with an Optronics MicroFire camera mounted on a Leica MZ16 stereomicroscope. From each recording, 10 frames were selected that represented the heart at various stages of contraction. In each frame, the angle of the atrium and ventricle from the sagittal plane was measured with NIH Image J 1.34 software (http://rsb.info.nih.gov/nih-image/), and these were averaged to yield an angle of looping for each heart.

Heart Function. The volume of the ventricle at end-diastole and end-systole and heart rate were measured in larvae to calculate stroke volume, ejection fraction, and cardiac output. The volume of the ventricle was approximated from linear dimensions taken from two-dimension images with Simpson's method, also called the method of discs (Schiller et al., 1989; Coucelo et al., 2000). This method approximates a ventricle volume by dividing the ventricle into slices of finite thickness from the apex to base and calculates the ventricle volume by addition of the individual slice volumes using the equation $V = \acute{O}_{i=1}^{n} A_i \times T$, where A is the planimetered area and T is the slice thickness. The two-dimensional image of each ventricle at end-diastole and end-systole was divided into 15 to 20 slices of 10 μm thickness. The planimeter area of each slice was calculated from its transverse diameter, which was assumed to be circular.

To generate a two-dimensional image of the ventricle at end-diastole and end-systole, time-lapse recordings were taken at 250 frames/s of the beating heart in larvae mounted in 3% methylcellulose with a MotionScope camera mounted on a Nikon TE300 inverted microscope. Frames that captured the ventricle at end-diastole and end-systole were identified and used to approximate the end-diastolic volume (EDV) and end-systolic volume (ESV). The ventricle was outlined in the selected frames, overlaid with a grid to designate the 10 μm divisions, and the transverse diameter recorded for each slice using MetaMorph software (Molecular Devices, Sunnyvale, CA). The same time-lapse recordings were used to calculate heart rate based on the number of frames between three beats.

Stroke volume (SV) and ejection fraction (EF) were calculated from the approximated EDV and ESV using the equations SV = EDV − ESV and EF = (EDV − ESV)/EDV × 100. Cardiac output (CO) was calculated from SV and heart rate (HR): CO = SV × HR.

Ventricle Size. Larvae were placed in 500 mM potassium chloride + 4 mg/ml Tricaine-S for 4 min to depolarize the cardiac myocytes resulting in a loss of excitability and cardiac arrest (Chambers, 2003). Larvae were immediately placed in 3% methylcellulose and the ventricle imaged with epifluorescence by a Micromax charge-coupled device camera (Princeton Scientific Instruments, Monmouth Junction, NJ) mounted on an inverted Nikon TE300 microscope. The volume of the arrested ventricle was calculated as described above.

Heart Myocyte Number. Cardiac myocytes were counted in *cmcl2*::*dsRed2-nuc* transgenic zebrafish larvae as described previously (Mably et al., 2003; Antkiewicz et al., 2005). Epifluorescence images were captured and the red fluorescent nuclei of the cardiac myocytes were counted to determine the number of cardiac myocytes.

Statistical Analysis. For blood flow, heart looping, pericardial sac area, EDV, ESV, HR, CO, EF, ventricle size, cardiac myocyte number, and real-time PCR quantitation of gene expression significance of TCDD-induced changes were determined using a two-way analysis of variance followed by the Fisher least-significant-difference test. These statistical analyses were performed using a Statistica 6.0 software package (StatSoft, Inc., Tulsa, OK). Results are presented as mean ± S.E.; level of significance was $p \leq 0.05$.

Results

Experimental Design. In previous studies of TCDD-induced cardiovascular toxicity, zebrafish embryos were exposed to TCDD shortly after fertilization; a point well before the onset of heart development (Henry et al., 1997; Dong et al., 2002; Teraoka et al., 2002; Prasch et al., 2003; Antkiewicz et al., 2005). However, to identify AHR/ARNT target genes, we needed to identify cardiac transcripts that were altered immediately after initial AHR activation by TCDD. To do this, we needed to expose the zebrafish during a window in which TCDD can induce cardiovascular toxicity and the hearts have developed to a stage that enabled extraction for RNA isolation. Previous work by Belair et al. (2001) showed that hatched larvae exposed to TCDD at 72 hpf had severely reduced blood flow by 120 hpf, indicating that 72 hpf is well within the window of sensitivity to TCDD-induced cardiovascular toxicity. Hearts can be readily extracted from zebrafish larvae from 72 to 84 hpf. Therefore, at 72 hpf, zebrafish larvae were exposed for 1 h to TCDD or vehicle, and then hearts were collected at 1, 2, 4, and 12 h after dosing (73, 74, 76, and 84 hpf, respectively) for microarray analysis (Fig. 1). It should be mentioned that TCDD is not appreciably redistributed or metabolized during this time course, so that TCDD was present in the tissues at all time points. The hearts were extracted as whole organs, including the four chambers connected in series (sinus venosus, atrium, ventricle, and bulbus arteriosus) with epicardial, myocardial, and endocardial layers. To provide a context for interpreting the TCDD-induced gene expression changes in the heart, we also assessed the progression of cardiovascular toxicity in larvae exposed to TCDD at 72 hpf.

Cardiovascular Toxicity in TCDD-Treated Zebrafish Larvae. The earliest toxic response observed was a decrease in ventricular stroke volume at 8 h after TCDD exposure (Fig. 2). We observed no consistent effect on heart rate; however, applying an algorithm previously validated in another fish species allowed us to assess the ventricular end-diastolic and end-systolic volumes using time-lapse recordings of the beating zebrafish hearts (Coucelo et al., 2000). This revealed a TCDD-induced decrease in stroke volume at 8 h (80 hpf). The decrease in stroke volume produced a concomitant decrease in cardiac output.

TCDD caused no change in the end-systolic volume but decreased the end-diastolic volume by 8 h (80 hpf) in TCDD-treated zebrafish larvae (Fig. 3). Therefore, the decrease in stroke volume and ejection fraction stems from the reduced end-diastolic volume caused by TCDD.

Peripheral blood flow, pericardial edema, and the heart loop structure were compared between vehicle and TCDD-treated larvae at 4, 12, 24, and 48 h after TCDD exposure (76, 84, 96, and 120 hpf) (Fig. 4). Within 12 h of exposure (84 hpf), TCDD caused a 30% reduction in blood flow through the intersegmental vessels of the trunk region, and by 48 h (120 hpf), flow had almost ceased (Fig. 4A). By 48 h (120 hpf), TCDD treatment also caused an increase in pericardial

edema (Fig. 4B) and altered the loop structure of the heart (Fig. 4C) that is characteristic of the late stages of heart failure in zebrafish embryos exposed to TCDD (Antkiewicz et al., 2005). The heart loop was examined as described under *Materials and Methods*, showing the angle of the atrioventricular axis to the sagittal plane (Fig. 4, top left image). Ventral view images of the heart in TCDD and vehicle-treated larvae (Fig. 4, representative images) clearly show the progression of cardiac toxicity from a normal well looped heart with a large angle in vehicle-treated larvae to an elongated, unlooped heart with a small angle and compacted chambers in TCDD-treated larvae.

To directly compare the sizes of the ventricles of TCDD and vehicle-treated larvae, potassium chloride was used to arrest the hearts for measurement. Direct measurement of the size of the ventricles revealed no difference in the relaxed ventricle volume of TCDD and vehicle-treated larvae at 12 h after treatment. By 24 h, however, TCDD had caused a significant reduction in the ventricle volume (Fig. 5A). Likewise, the number of cardiac myocytes was not significantly reduced by TCDD until the 24 h point (Fig. 5B).

It seems that TCDD halted growth of the heart at a point around 12 h after exposure. This is suggested by the fact that although the control hearts increased in size and cell number in the interval between the 12- and 24-h time points (84 to 96 hpf), the TCDD-treated hearts did not. The size of the ventricle and the number of cardiac myocytes in the hearts of TCDD-treated larvae at 24 h after exposure is about the same as observed at the 12-h point for both TCDD-treated and untreated larvae.

TCDD-Induced Transcriptional Response in the Heart. TCDD-induced gene expression changes in the heart were identified at all points examined, 1, 2, 4, and 12 h after TCDD exposure. Many of these changes preceded any observed change in heart morphology and function, whereas other sets of gene expression changes were correlated with the emergence of cardiac toxicity. Expression of 160 genes

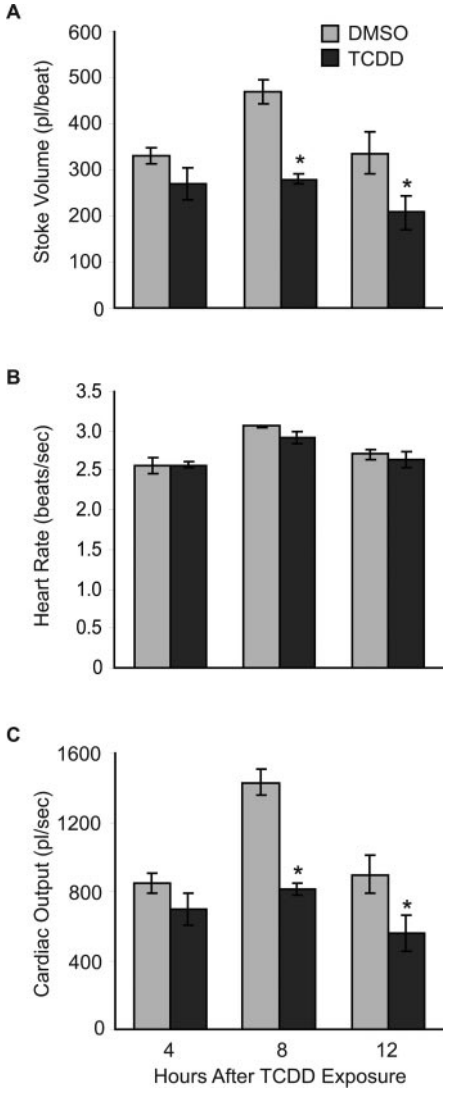

Fig. 2. Cardiac function is reduced within 12 h in zebrafish larvae exposed to TCDD. Larvae were exposed to TCDD or vehicle for 1 h at 72 hpf, and the beating heart was imaged with time-lapse recordings at 4, 8, and 12 h after exposure (76, 80, and 84 hpf). A, stroke volume was calculated from EDV and ESV values approximated from two-dimensional images of the ventricle at end-diastole and end-systole. B, heart rate was calculated from the number of frames between three consecutive heart beats in the time-lapse recordings. C, cardiac output was calculated from stroke volume and heart rate. Values are mean ± S.E. of $n = 5$. *, significant difference between TCDD (1 ng/ml) and its respective vehicle control (0.1% DMSO) for each time point ($p \leq 0.05$).

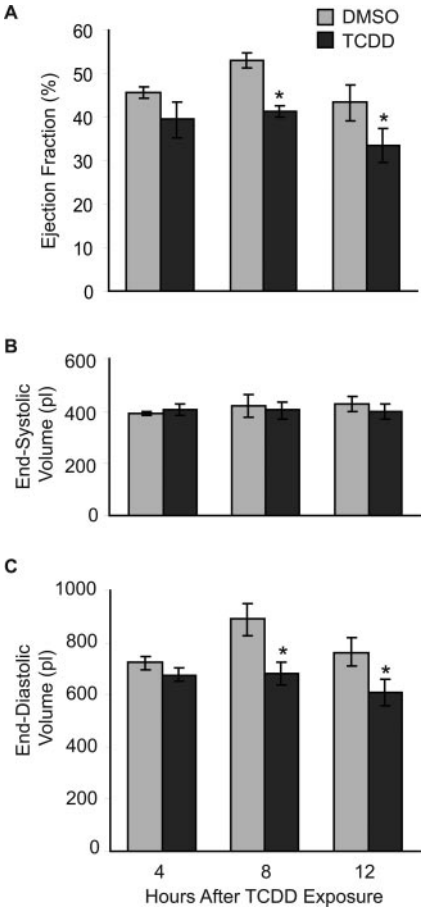

Fig. 3. Contribution of TCDD-induced changes in EDV and ESV to altered ejection fraction in larvae exposed to TCDD. Larvae were exposed to TCDD or vehicle for 1 h at 72 hpf, and the beating heart was imaged with time-lapse recordings at 4, 8, and 12 h after exposure (76, 80, and 84 hpf). A, ejection fraction was calculated from EDV and ESV. B, ESV was approximated from a two-dimensional image of the ventricle at end-systole. C, EDV was approximated from a two-dimensional image of the ventricle at end-diastole. Values are mean ± S.E. of $n = 5$. *, significant difference between TCDD (1 ng/ml) and its respective vehicle control (0.1% DMSO) for each time point ($p \leq 0.05$).

was changed 2-fold or more by TCDD exposure at one or more of these time points. Hierarchical clustering placed these transcripts into groups with similar TCDD-induced patterns of expression (Fig. 6A). At first, TCDD induced up-regulation of a small group of 19 genes at 1 h after TCDD exposure (73 hpf). The most strongly up-regulated of those genes fall into cluster 1, which is mostly composed of genes encoding xenobiotic metabolizing enzymes, cytochrome P450 1a, cytochrome P450 1b, and cytochrome P450 1c1, as well as myeloid-specific peroxidase and a transcript similar to a novel TCDD-inducible poly (ADP-ribose) polymerase (Fig. 6A, Table 1). Expression of the genes in clusters 1, 2, 3, 7, and 8 was altered within 1 to 2 h of TCDD activation of the AHR pathway (Fig. 6A); therefore, these genes are the strongest candidates for being AHR/ARNT targets. These transcriptional responses to TCDD precede the development of cardiac toxicity in zebrafish larvae and, except for the genes encoding xenobiotic metabolizing enzymes, they function mostly in cellular signaling pathways and transcriptional regulation (Fig. 6B). The data for these early responding genes, meeting the criterion of being up-regulated at either the 1- or 2-h point, are listed in Table 2.

The first three sets of samples for microarray analysis were collected at times that preceded observable TCDD-induced cardiac toxicity, which did not appear until 8 h after exposure. The great majority of expression changes at these time points (1–4 h after exposure) were positive, representing genes that are up-regulated by TCDD. However, the samples collected during the onset of toxicity at the 12-h point (84 hpf) revealed a large cluster of 76 transcripts that were down-regulated in hearts of TCDD-treated larvae (Fig. 6A, cluster

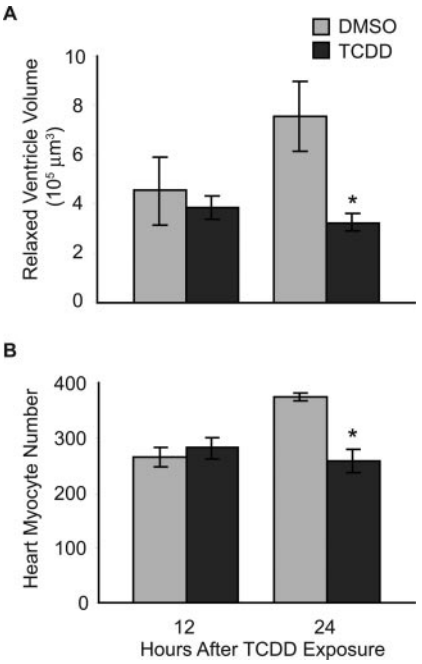

Fig. 5. Effect of TCDD exposure on heart size in developing zebrafish larvae. Larvae were exposed to TCDD or vehicle for 1 h at 72 hpf and assessed at 12 and 24 h (84 and 96 hpf). A, the volume of the ventricle was approximated from two-dimensional images captured after treatment with potassium chloride to arrest the heart. B, the number of cardiac myocytes was counted in epifluorescent images of flat-mounted *cmcl2*::*deRed2-nuc* transgenic larvae. Values are mean ± S.E. of $n = 5$. *, significant difference between TCDD (1 ng/ml) and its respective vehicle control (0.1% DMSO) for each time point ($p \leq 0.05$).

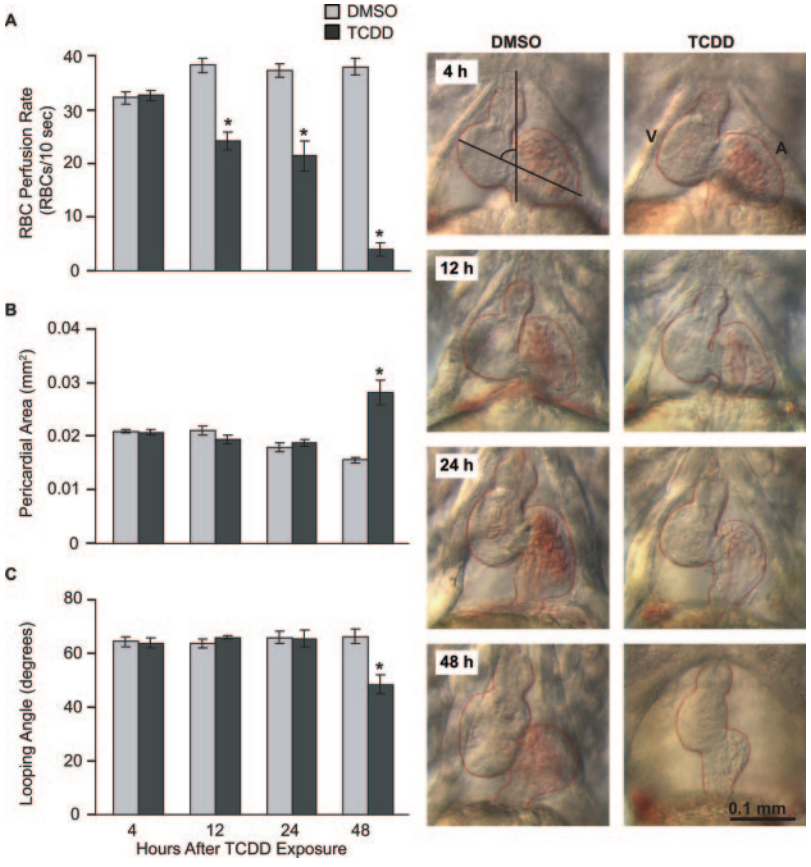

Fig. 4. TCDD exposure at 72 hpf causes cardiovascular toxicity in zebrafish larvae. Larvae were exposed to TCDD or vehicle for 1 h at 72 hpf and assessed for endpoints of cardiovascular toxicity at 4, 12, 24, and 48 h after exposure (76, 84, 96, and 120 hpf). A, red blood cell perfusion rates were measured in an intersegmental vessel posterior to the anal pore as an index of peripheral blood flow in larvae from each treatment group. B, pericardial area was measured from lateral view images of the pericardial sac area as an index of pericardial edema in larvae from each treatment group. C, the angle of the longest plane through the ventricle and atrium bisecting the atrioventricular valve from the sagittal plane was measured as an index of heart looping. Images at the right are representative photos of the ventral view of the heart depicting heart looping at 4, 12, 24, and 48 h after exposure to TCDD (1 ng/ml) or vehicle control (0.1% DMSO). Values are mean ± S.E. of $n = 10$. *, significant difference between TCDD and its respective vehicle control for each time point ($p \leq 0.05$). Scale bar, 0.1 mm.

9). More than half of these genes are involved in cell division and proliferation (Fig. 6B, cluster 9) and function in DNA synthesis, replication, and repair; cell cycle control; chromosome condensation; mitotic spindle formation; and cytokinesis (Table 3 and Supplemental Table S1). These gene expression changes coincide with the onset of TCDD-induced cardiac toxicity and reduced peripheral blood flow. Therefore, they may be secondary consequences of earlier TCDD-induced transcriptional changes. They may also be homeostatic responses to TCDD-induced cardiac toxicity and ischemia. In addition to the genes controlling cell division and proliferation, TCDD exposure altered expression of genes that encode proteins involved in ion movement, calcium modulation, contractile function, and cell adhesion (Table 4 and Supplemental Table S1), processes that are necessary for normal myocyte contraction. TCDD also altered expression of genes from signaling pathways and transcription factors that play essential roles in normal heart development in zebrafish. These include members of the Notch and transforming growth factor-β signaling pathways and transcription factors that control muscle-specific genes (Table 4 and S1).

Real-time quantitative PCR of selected genes was conducted to confirm the trends and patterns of the TCDD-induced transcriptional response in the zebrafish heart. TCDD-induced expression levels for each gene selected for real-time PCR analysis were normalized to β-actin, the expression of which was not altered by TCDD treatment during this time course. The results of the real-time PCR analysis are shown in bold in Tables 1 to 4 and confirm the TCDD-induced up-regulation or down-regulation of those genes in the zebrafish heart.

Comparison of TCDD-Induced Transcriptional Response in the Heart Versus Body. At each time point, the bodies of zebrafish larvae were also collected after removal of the hearts to allow microarray comparisons using extracardiac tissue. The set of genes altered 2-fold or greater by TCDD, in either the bodies or hearts, at any time point were organized by expression pattern using hierarchical clustering (Fig. 7A). Beyond a group of genes up-regulated across the time course by TCDD that consists mostly of genes encoding phase I and II metabolizing enzymes (Fig. 7A, lower box), there was little similarity in the transcriptional response to TCDD in the heart and body samples. There were fewer TCDD-induced up-regulated genes detected in the

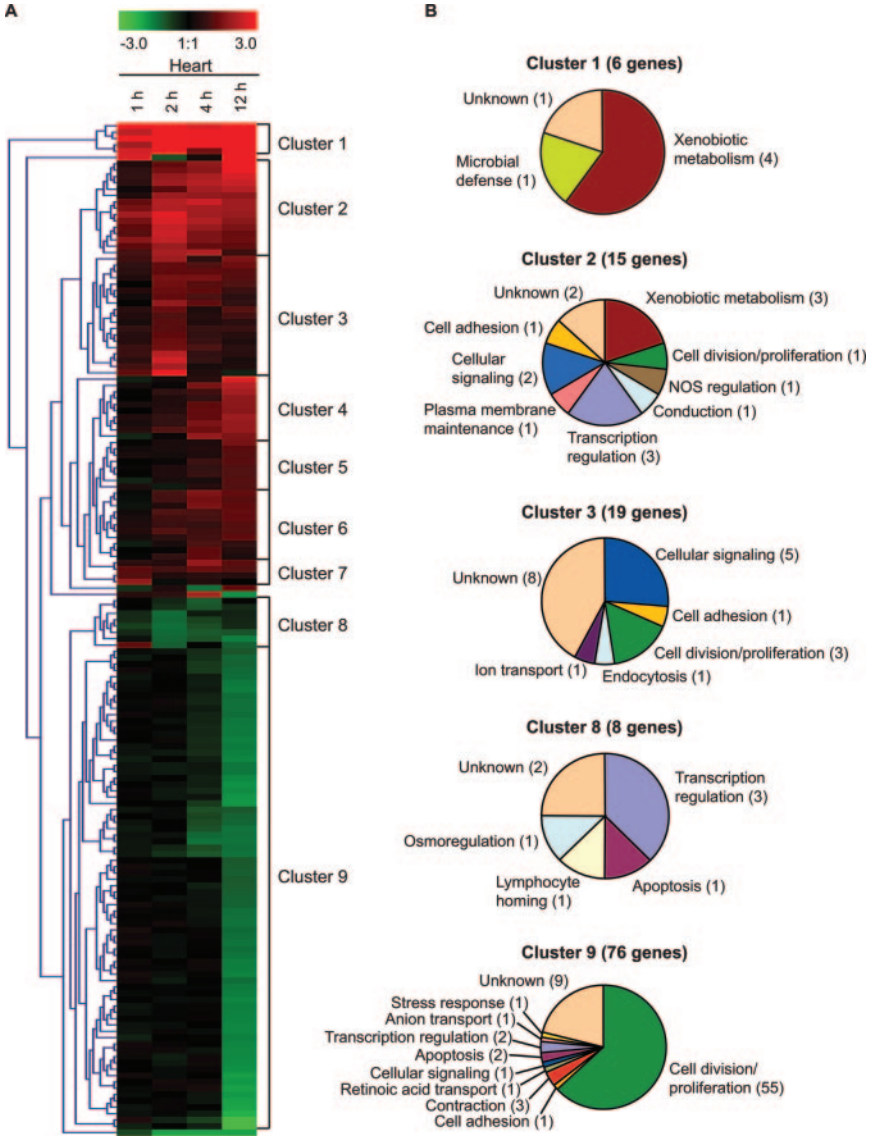

Fig. 6. Clustering of TCDD-induced gene expression changes in the zebrafish heart. Larvae were exposed to TCDD or vehicle for 1 h at 72 hpf, and hearts were collected for microarray analysis at 1, 2, 4, and 12 h after initial exposure (73, 74, 76, and 84 hpf). A, hierarchical cluster of genes which TCDD significantly altered expression $\geq$2-fold at any time point. B, pie charts show biological functions of genes in clusters 1, 2, 3, 8 (pretoxicity gene expression changes), and 9 (post-toxicity gene expression changes).

whole-body samples compared with the heart samples across all time points. Furthermore, the large cluster of genes down-regulated in the heart at the 12-h point (84 hpf) was not detected in the body samples (Fig. 7B). Most of the TCDD-induced gene expression changes detected in the body samples were also present in the heart samples, but most of the

TABLE 1
Time course of TCDD-induced gene expression changes associated with xenobiotic metabolism in the heart of zebrafish larvae
Bold values represent real-time PCR results.

Affymetrix ID	Gene Title	Log_2 (TCDD/DMSO)			
		1 h	2 h	4 h	12 h
Sensor					
Dr0.8105.1.S1_at	Aryl hydrocarbon receptor 2	NC	NC	1.5	1.2
Phase I metabolism					
Dr0.9478.1.S1_at	Cytochrome P450 1a	3.3	3.9	2.3	5.5
		4.6	**7.9**	**6.9**	**7.0**
DrAffx0.2.86.S1_at	Cytochrome P450 1b1	3.3	4.1	4.2	3.4
DrAffx0.2.87.S1_at	Similar to cytochrome P450 1c1	2.2	4.9	4.5	5.3
Dr0.25208.1.A1_at	Cytochrome P450 3a65	NC	1.9	2.2	2.4
Phase II metabolism					
Dr0.3583.1.S1_at	Sulfotransferase	1.2	2.2	2.4	1.9
Dr0.5410.1.A1_at	Similar to UDP-glucuronosyltransferase	NC	1.0	1.3	1.8
Dr0.22620.1.S1_at	Similar to glutathione *S*-transferase θ-1	NC	NC	NC	1.2

NC, no significant change above 2-fold.

TABLE 2
Genes up-regulated in the heart of zebrafish larvae 1 to 2 h after TCDD exposure

Affymetrix ID	Genbank Accession No.	Gene Title	Log_2 (TCDD/DMSO)			
			1 h	2 h	4 h	12 h
Cluster 1						
Dr0.9478.1.S1_at	NM_131879	Cytochrome P450 1a	3.3	3.9	2.9	5.5
DrAffx0.2.87.S1_at	AL918492	Cytochrome P450 1c1	2.2	4.9	4.5	5.3
DrAffx0.2.86.S1_at	AY534681	Cytochrome P450 1b1	3.3	4.1	4.2	3.4
Dr0.5536.1.A1_at	BG306468	Similar to TCDD-inducible poly(ADP-ribose) polymerase	1.9	3.5	2.9	2.9
Dr0.9478.2.S1_at	NM_212779	Myeloid-specific peroxidase	2.5	2.7	1.4	2.8
Cluster 2						
Dr0.18724.1.A1_at	AI721597	Similar to CXXC finger 5	NC	1.9	1.8	1.7
Dr0.17164.1.A1_at	BI982814	Similar to hypothetical protein MGC33926	NC	1.1	1.9	2.1
Dr0.25208.1.A1_at	AY452279	Cytochrome P450 3a65	NC	1.9	2.2	2.4
Dr0.21790.1.A1_at	NM_212571	Protocadherin 10a	NC	1.8	2.0	2.5
Dr0.5040.1.S1_at	BC053263	Similar to cytochrome b_5	NC	1.4	1.6	2.8
Dr0.2499.1.S1_at	BC078421	Myogenin	NC	1.2	1.7	2.9
Dr0.8093.1.S1_at	BC066679	Paraxis	NC	2.0	2.1	NC
Dr0.9917.1.S1_at	BC047851	Glutamate decarboxylase 1	1.2	1.8	1.3	1.2
Dr0.26003.1.A1_at	CD605928		1.6	2.3	1.5	1.3
Dr0.5428.2.A1_at	NM_201143	Similar to phosphoinositide-3-kinase, regulatory subunit, polypeptide 3 (p55, γ)	1.1	2.4	1.5	1.3
Dr0.12454.1.S1_at	NM_200762	GTP cyclohydrolase I feedback inhibitor	1.2	2.3	1.8	1.5
Dr0.9896.1.A1_at	BI670851	Similar to serum/glucocorticoid kinase[a]	1.5	2.6	2.1	1.7
Dr0.13774.1.S1_at	BI703179	Similar to sphingosine 1-phosphate receptor Edg-3[a]	1.9	2.7	1.9	1.8
Dr0.25740.1.A1_at	NM_199644	Similar to ADP-ribosylation factor 4-like	1.4	2.1	2.0	1.9
Dr0.3583.1.S1_at	NM_214686	Sulfotransferase	1.2	2.2	2.4	1.9
Cluster 3						
Dr0.25257.1.A1_at	CD014962	Similar to enhancer-of-split and hairy-related protein[a]	NC	1.9	NC	1.5
Dr0.1917.1.A1_at	AW567374	Max interacting protein 1	NC	1.2	1.0	1.3
Dr0.12687.1.A1_at	AI793557	Similar to growth arrest-specific 2 like 1	NC	1.2	1.2	1.1
Dr0.7603.1.A1_at	NM_199980	Similar to integral membrane protein 2C	NC	1.4	1.5	1.1
Dr0.7683.1.A1_at	BQ264112	Similar to synaptojanin 1[a]	NC	1.4	1.1	1.0
Dr0.14573.2.A1_at	NM_205663	Similar to lipoma HMGIC fusion partner	NC	1.3	1.6	NC
Dr0.22000.1.A1_at	AI957705		NC	1.0	NC	NC
Dr0.3021.2.S1_at	BQ617923	Similar to regulator protein p122-RhoGAP	NC	1.1	NC	NC
Dr0.17890.1.S1_at	BC068370	Similar to claudin 5	NC	1.1	NC	NC
Dr0.11465.1.A1_at	AW777449	Similar to HIF-prolyl hydroxylase 2	NC	1.2	NC	NC
Dr0.8120.1.S1_at	AF159147	Noggin 1	NC	1.3	NC	NC
Dr0.5129.1.S1_at	NM_213519	Similar to human sestrin 3	NC	1.4	1.0	NC
Dr0.16163.1.S1_at	NM_205626	BCL6 co-repressor	NC	2.2	NC	NC
Dr0.17146.1.A1_at	BM102517		NC	2.5	NC	NC
Dr0.13289.1.A1_at	BI886117		NC	2.0	NC	NC
Dr0.11351.1.A1_at	NM_200789		1.2	2.9	NC	NC
Cluster 7						
Dr0.4076.1.S1_at	NM_131519	Endothelin 1	1.1	NC	1.3	1.1
Dr0.431.1.S1_at	BC059551	Hairy-related 6	1.1	NC	NC	NC
Dr0.10713.1.S1_at	NM_131688	ATPase, Na^+/K^+ transporting, α 1a0.3 polypeptide	1.7	NC	NC	NC

[a] Probe blasts to 3′-untranslated region of indicated gene.
NC, no significant change above 2-fold.

expression changes detected in the heart samples were not detected in the extracardiac tissues (Fig. 7B).

Discussion

Our hypothesis is that TCDD produces toxicity in zebrafish hearts through organ-specific transcriptional activation of AHR/ARNT target genes. The availability of zebrafish microarrays makes it practical to search for these targets among a very large set of potential transcripts. However, there were two obstacles to overcome. First, because direct AHR activation of target genes would be expected to cause many secondary downstream responses, culminating in overt heart failure, it was not sufficient to measure transcript changes at the time of the toxic response. Such an experiment cannot distinguish primary TCDD-mediated transcriptional changes from secondary and tertiary effects. Indeed there is no guarantee that the transcripts directly regulated by ligand activated AHR/ARNT are still altered at the time of full-blown cardiac toxicity. By following the time course of transcriptional changes starting immediately after TCDD exposure through to initial stages of cardiovascular toxicity, we would be able to identify transcript sets that are the first to respond to TCDD. These early responding genes are likely to be AHR/ARNT targets and putative mediators of cardiac toxicity. We needed to identify a time in zebrafish development at which the heart was formed and removable in sufficient numbers for RNA hybridization yet still sensitive to the developmental effects of TCDD. We found that a novel heart extraction method (Burns and MacRae, 2006) and 72 hpf zebrafish were ideal for this.

There were several striking aspects to our results. First, the almost immediate induction of the genes in the AHR battery in both heart and body samples indicated rapid TCDD activation of AHR in the heart tissue. Second, in the heart, we observed the expected early induction of a relatively small set of genes, followed by larger transcript clusters as time progressed. Third, with the exception of the small cluster of xenobiotic metabolizing genes, the majority of gene expression changes observed in the heart were not characteristic of zebrafish cells in general and were not observed in the body samples. Thus, in contrast to the majority of the surrounding tissues, the developing heart stands out as an organ in which TCDD induces both toxicity and changes in gene expression. Finally, the known functions of many of the transcripts altered in the heart by TCDD exposure are consistent with the nature and timing of TCDD-induced cardiotoxic responses.

TCDD Rapidly Induced a Cluster of Xenobiotic Metabolizing Genes in Both Heart and Body Samples. Genes in cluster 1 (Fig. 6A) encode xenobiotic metabolizing

TABLE 3

Time course of TCDD-induced gene expression changes associated with myocyte cell number hearts of zebrafish larvae

See supplemental microarray data for the full list of cell division/proliferation genes down-regulated by TCDD. Bold values represent real-time PCR results.

Affymetrix ID	Genbank Accession No.	Gene Title	Log_2 (TCDD/DMSO)			
			1 h	2 h	4 h	12 h
Cell division/proliferation						
Dr0.5428.2.A1_at	BG304105	Phosphoinositide-3-kinase	1.1	2.4	1.5	1.3
		regulatory subunit, polypeptide 3 (p55, γ)	**0.9**	**1.1**	**NC**	**NC**
Dr0.5129.1.S1_at	BC045518.1	Similar to sestrin	NC	1.4	1.0	NC
Dr0.12687.1.A1_at	AI793557	Similar to growth arrest-specific 2-like 1 isoform a	NC	1.2	1.2	1.1
Dr0.1917.1.A1_at	AW567374	Max-interacting protein 1	NC	1.2	1.0	1.3
Dr0.15237.1.A1_at	BM185827	Similar to brain-specific angiogenesis inhibitor 1	NC	NC	1.8	1.0
Dr0.20177.1.A1_at	AI793650	Similar to tumor protein p53-binding protein 1	NC	NC	1.2	1.6
Dr0.5408.1.S1_at	BC046050.1	RAD54-like	NC	NC	NC	−2.0
Dr0.17623.1.S1_at	BQ074593	Forkhead box M1-like	NC	NC	NC	−1.9
Dr0.24379.1.S1_at	AF268044.1	Cell division cycle 2	NC	NC	NC	−1.8
Dr0.7155.2.S1_a_at	BM342138	Nucleolar and spindle-associated protein 1	NC	NC	NC	−1.8
Dr0.377.1.S1_at	BC047856.1	Primase polypeptide 1	NC	NC	NC	−1.7
Dr0.25190.1.S1_at	NM_152949.1	Cyclin A2	NC	NC	NC	−1.6
Dr0.2833.1.A1_at	AW154091	Similar to cell division cycle-associated 3	NC	NC	NC	−1.6
Dr0.6360.1.A1_at	BQ616864	Similar to cytoskeleton-associated protein 2	NC	NC	NC	−1.6
Dr0.25226.1.S1_s_at	NM_131513.1	Cyclin B1	NC	NC	NC	−1.5
Dr0.1348.1.S1_at	NM_131404.1	Proliferating cell nuclear antigen	NC	NC	NC	−1.5
			NC	**−0.7**	**−1.7**	**−1.5**
Dr0.20131.4.S1_at	AW116681	Polo-kinase 1	NC	NC	NC	−1.5
Dr0.25652.1.S1_at	AL715042	Kinetochore-associated 2-like	NC	NC	NC	−1.5
Dr0.11651.1.S1_at	NM_178436.2	Minichromosome maintenance-deficient 5	NC	NC	−1.4	−1.4
Dr0.2291.1.S1_at	NM_173257.1	Minichromosome maintenance-deficient 2	NC	NC	−1.2	−1.4
			NC	**NC**	**−2.5**	**−1.5**[c]
Dr0.1294.1.S1_at	BC049413.1	Flap structure-specific endonuclease 1	NC	NC	NC	−1.4
Dr0.24945.1.S1_at	AI332229	Origin recognition complex subunit 6 homolog-like	NC	NC	NC	−1.4
Dr0.1691.1.S1_at	NM_131450.1	Ribonucleotide reductase M2 polypeptide	NC	NC	NC	−1.4
Dr0.20010.4.S1_at	BI704246	Cell division cycle associated 8-like	NC	NC	NC	−1.3
Dr0.4556.1.S1_at	NM_131711.1	Replication protein A2	NC	NC	NC	−1.3
Dr0.1514.1.A1_at	CB361060	RAD51 homolog	NC	NC	NC	−1.3
Dr0.15472.1.S1_at	NM_175042.2	Monopolar spindle 1	NC	NC	NC	−1.1
Dr0.14405.1.S1_at	AY277636.1	Proliferation-associated nuclear element	NC	NC	NC	−1.0
Apoptosis						
Dr0.13050.1.S1_at	BI882315	Similar to tumor-suppressing subtransferable candidate 3	NC	−1.3	NC	NC
Dr0.20391.1.A1_at	AI878653	Similar to novel apoptosis-stimulating of p53	NC	NC	NC	1.2
Dr0.15033.1.S1_at	BM571671	Similar to human protein p8	NC	NC	NC	1.1
Dr0.13740.1.S1_at	BI866919	Similar to apoptosis-inducing TAF9-like domain 1	NC	NC	NC	−1.4
Dr0.14671.1.S1_at	AY057057.1	Baculoviral IAP repeat-containing 5a	NC	NC	NC	−1.1

NC, no significant change above 2-fold.

enzymes, including cytochrome P4501a, cytochrome P4501b1, and cytochrome P4501c1, as well as myeloid-specific peroxidase and a transcript similar to a novel TCDD-inducible poly (ADP-ribose) polymerase. Most of these were induced during the first hour of TCDD exposure in both heart and body samples. This cluster contains genes that are known direct targets for AHR and were therefore very likely to have been directly induced by AHR/ARNT binding to promoter elements. Although our study looked specifically at only one tissue type, the fact that this cluster of xenobiotic metabolizing genes was induced in both the heart and the extracardiac samples is consistent with the idea that the xenobiotic protective function may be widespread in cells expressing AHR and ARNT.

Temporal Patterns of Gene Expression in Heart and Extracardiac Tissues. Beyond the small cluster of xenobiotic metabolizing transcripts, the pattern of the transcriptional response in the heart was quite distinct from that in extracardiac tissues. The number of genes affected in the heart steadily increased, whereas the number of transcripts altered in the body samples remained relatively constant throughout the time course. In addition, the early changes in the heart samples were primarily gene induction events, but by 12 h after exposure, there was a large cluster of down-regulated heart transcripts. Given the fact that AHR/ARNT has been characterized as a transcriptional activator, the down-regulation of these genes may be a secondary response to earlier transcriptional changes. This pattern is consistent with a cascade of events, in which early activation of a small set of genes by AHR/ARNT leads to progressive cellular changes. Indeed, although the transcriptional effects of TCDD continued to increase over time, at 12 h after exposure, many of the initial transcriptional changes had diminished or disappeared.

Gene clusters 2 and 3 contained a group of genes that were rapidly altered in the heart, but were unaffected in the body samples. These clusters consisted largely of genes involved in controlling cellular growth, development, and homeostasis; such changes would be expected to have profound effects on heart cell growth and development.

Cluster 9 was even more striking in that it consisted of a heart-specific set of 71 transcripts down-regulated at 12 h after TCDD exposure (84 hpf). Another important feature about this gene cluster is that more than 70% of the genes in this cluster are involved in cell cycle progression.

Mechanisms of Cardiac Gene Regulation. Our results do not clearly distinguish transcripts that are directly regulated by AHR activation from those that are indirectly affected. However, TCDD very rapidly induced known AHR targets such as *cyp1a* in the heart cells. In this case, the changes are most easily explained by direct AHR/ARNT activation within the cardiac cells. In addition, the rapidity of the transcriptional response in the heart cells, occurring within an hour of TCDD exposure and hours before any perceptible hemodynamic change, argues against regulation of the early transcripts through indirect effects mediated by other cell types or as responses to physiological changes in blood flow.

TABLE 4
Time course of TCDD-induced gene expression changes associated with heart development and function in zebrafish larvae
Bold values represent real-time PCR results.

Affymetrix ID	Gene Title	Log_2 (TCDD/DMSO)			
		1 h	2 h	4 h	12 h
Ion regulation					
Dr0.13774.1.S1_at[a]	Similar to sphingosine 1-phosphate receptor Edg-3[b]	1.9	2.7	1.9	1.8
Dr0.9896.1.A1_at	Similar to serum/glucocorticoid regulated kinase[b]	1.5	2.6	2.1	1.7
Dr0.10713.1.S1_at	Na^+/K^+ ATPase α1a3 polypeptide	1.7	NC	NC	NC
Dr0.9878.1.S1_at	Na^+/K^+ ATPase α3b polypeptide	NC	NC	1.5	1.7
		NC	**1.5**	**3.5**	**3.0**
Dr0.14133.1.S1_at	Similar to K^+ channel tetramerization domain	NC	1.3	NC	1.1
Dr0.3021.2.S1_at	Similar to regulator protein p122-RhoGAP	NC	1.1	NC	NC
Dr0.1435.1.S1_at	Caveolin 3	NC	NC	1.2	1.9
Contractility					
Dr0.4076.1.S1_at	Endothelin 1	1.1	NC	1.3	1.1
		1.6	**0.5**	**1.0**	**1.0**
Dr0.12454.1.S1_at	GTP cyclohydrolase I feedback inhibitor	1.2	2.3	1.8	1.5
Dr0.6237.1.S1_at	Kinesin family member C1	NC	NC	NC	−1.9
Dr0.15087.1.A1_at	Protein kinase C beta 1	NC	NC	NC	−1.0
Notch signaling					
Dr0.431.1.S1_at	Hairy-related 6	1.1	NC	NC	NC
Dr0.25257.1.A1_at	Similar to enhancer-of-split and hairy-related protein 1	NC	1.9	NC	1.5
Dr0.8232.1.S1_at	Hairy/enhancer-of-split related with YRPW	NC	−1.2	NC	NC
	Motif 2	NC	−1.2	NC	NC[c]
TGF-β signaling					
Dr0.8120.1.S1_at	Noggin 1	NC	1.3	NC	NC
Dr0.25506.1.A1_at	Bmp receptor type 1a	NC	NC	NC	−1.3
Dr0.15495.1.A1_at	Similar to bmp 6 precursor	NC	NC	1.4	1.1
Myogenesis and muscle-specific gene regulation					
Dr0.25775.1.S1_at	Iroquois homeobox protein 4a	NC	NC	−1.1	NC
		NC	**NC**	**NC**	**0.7**
Dr0.2499.1.S1_at	Myogenin	NC	1.2	1.7	2.9
		NC	**NC**	**NC**	**1.6**
Dr0.8093.1.S1_at	Paraxis	NC	2.0	2.1	NC

[a] GenBank accession number BI703179.
[b] Probe blasts to 3′-untranslated region of indicated gene.
NC, no significant change above 2-fold.

The causes of later transcriptional changes in the heart are far more uncertain. As indicated, many of these are decreases in transcript abundance and may be secondary responses. Circulation has dropped at 12 h after TCDD exposure, and it is possible that tissues such as the peripheral vascular endothelium produce signals eliciting some of gene expression changes observed in heart cells at this later time point.

Heart versus Body. The transcriptional response to TCDD was remarkably different between the heart and body samples. However, it must be borne in mind that the gene expression changes measured in the bodies represent the average of the changes in a variety of tissues. This averaging effect may mask TCDD-induced transcript changes that occur in an organ or cell type that makes up only a small fraction of the tissue. Despite these uncertainties, the TCDD-induced pattern of transcript changes in the heart is clearly quite distinct from that produced in the body samples, where the xenobiotic metabolism response was predominant. This indicates that different cell or tissue types can have very distinct transcriptional responses to TCDD activation of AHR. It will be interesting to determine whether other TCDD-responsive tissues have characteristic transcriptional responses.

A set of microarray experiments examining the effects of TCDD on gene expression in the murine fetal heart has recently been reported (Thackaberry et al., 2005a). In this work, the authors discuss the lack of concordance between sets of genes identified in different published microarray experiments examining responses to TCDD. In a general sense, TCDD induced a similar set of xenobiotic metabolism genes in the mouse and zebrafish hearts. However, there were not strong similarities in the datasets. This probably stems in part from the major differences in the design of the experiments, in which we closely concentrated on the time

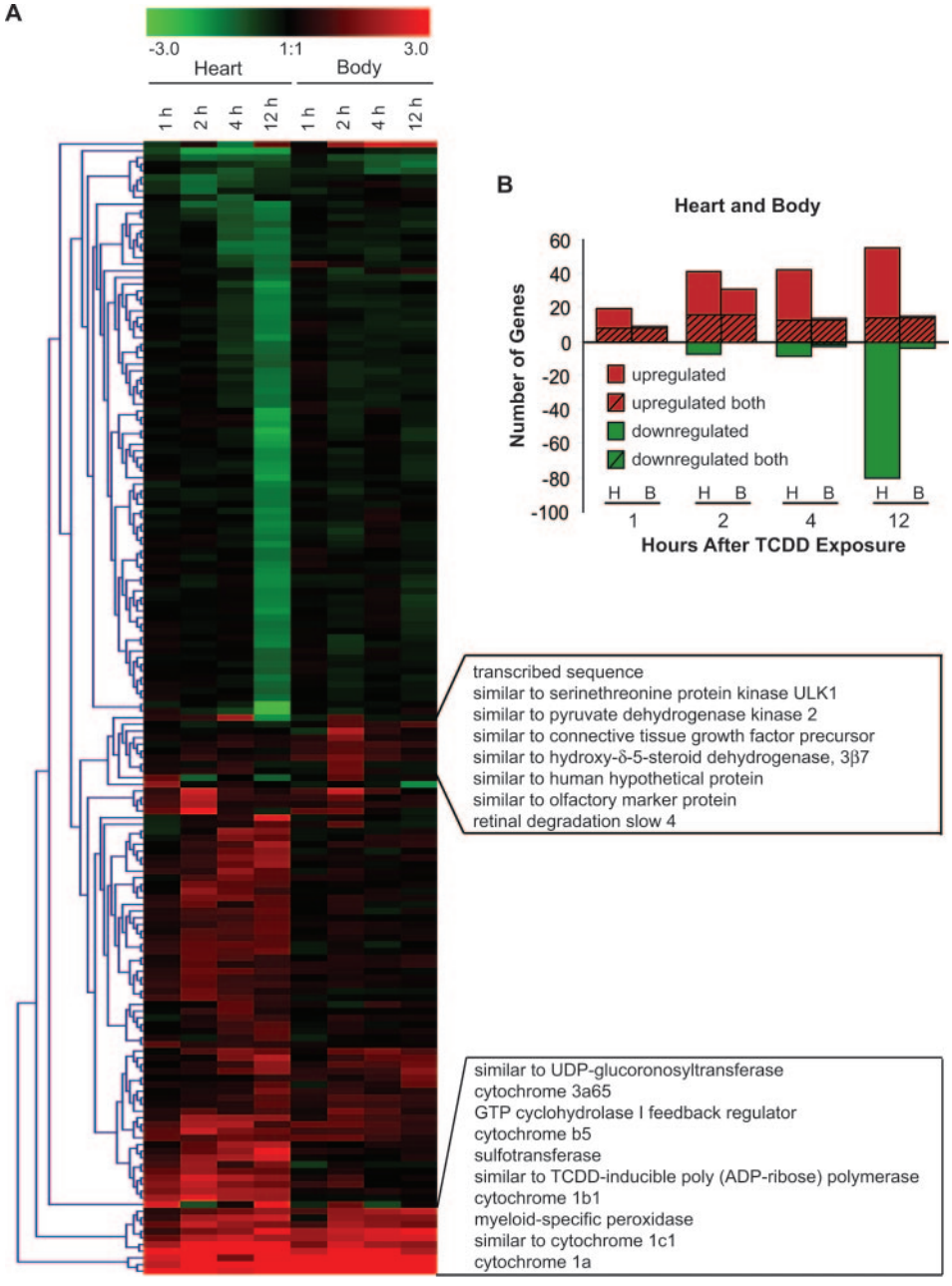

Fig. 7. Comparison of TCDD-induced gene expression changes in the zebrafish heart and whole body. Larvae were exposed to TCDD or vehicle for 1 h at 72 hpf, and hearts, as well as samples of bodies with hearts removed, were collected for microarray analysis at 1, 2, 4, and 12 h after initial exposure (73, 74, 76, and 84 hpf). A, hierarchical cluster of genes in which TCDD significantly altered expression by ≥2-fold in either the heart or body samples at any time point. B, number of genes up- or down-regulated 2-fold or more in the heart or body by TCDD exposure. The left column at each time point represents the number of genes significantly up-regulated (red) or down-regulated (green) in the heart (H), whereas the right column at each time point represents changes in the body (B). The hashed portion of each column represents the number of significantly altered genes found in both the heart and body samples, illustrating the amount of overlap in the genes regulated by TCDD in both heart and body.

frame after exposure. Furthermore, developing fish are substantially more sensitive to developmental abnormalities caused by AHR activation than mammals (Elonen et al., 1998).

Heart-Specific Physiological Responses. A common approach to studying the developmental effects of TCDD in zebrafish has been to expose embryos immediately after fertilization (Henry et al., 1997; Teraoka et al., 2002; Antkiewicz et al., 2005). The exposed embryos develop normally through gastrulation and early heart formation but then steadily exhibit signs of cardiotoxicity over the next few days (Antkiewicz et al., 2005). When larvae were exposed to TCDD after formation of the heart at 72 hpf, the cardiovascular response to AHR activation was clear cut, with signs of toxicity manifested after only 8 h of exposure (80 hpf). The two major responses observed were decreased end-diastolic volume (EDV) and a reduction in cardiomyocyte numbers. These were first observed at 8 and 24 h after exposure, respectively.

The decrease in EDV could be due to a decrease in the force of blood filling the ventricle or to a decrease in the ability of the ventricle to relax and dilate between contractions. There is precedence for the first model in that TCDD has been shown to increase vascular permeability in fish (Guiney et al., 2000; Dong et al., 2004). Proteins leaking from the blood into the intracellular space would decrease blood volume and central venous pressure.

Relaxation of the ventricle during diastole depends largely on the distensibility of the ventricle and clearing of Ca^{+2} from the cytosol. Myocytes relax when Ca^{+2} is sequestered into the sarcoplasmic reticulum or extruded to the intercellular space to prepare for the next contraction. In zebrafish embryo hearts, impaired extrusion of Ca^{+2} from the cytosol results in defects in ventricle contraction and heart morphology (Ebert et al., 2005). Therefore, impairment of this mechanism or an increase in ventricle rigidity could reduce ventricular expansion during filling. The tight coupling between cardiac output and venous return makes it difficult to determine, based only on the heart function measurements examined, whether reduced filling or impaired ventricle relaxation caused the decrease in EDV. However, it is interesting to note that several genes needed for the maintenance of normal ionic balance and contractility were found among the early sets of transcripts altered by TCDD exposure.

Studies with mice, chicks, and fish suggest that regulation of cardiac myocyte proliferation is a key mechanism by which AHR alters heart growth during development (Ivnitski et al., 2001; Lin et al., 2001; Thackaberry et al., 2003, 2005a,b; Antkiewicz et al., 2005). Possible mechanisms include transcriptional regulation of genes that control proliferation as well as direct interactions between AHR and cell cycle regulatory proteins in the nucleus (Puga et al., 2000a,b). In our experiments, the reduction in cardiomyocyte number might also be secondary to reduced cardiac output because heart function and growth are tightly linked (Hove et al., 2003). However, gene expression changes that would inhibit heart cell proliferation were observed well before TCDD-induced heart dysfunction. For example, during the first 2 h of exposure, TCDD up-regulated two negative regulators of cell cycle progression: phosphoinositide-3-kinase polypeptide 3 p55 γ (pik3r3) and max interacting protein 1 (mxi1). Pik3r3 binds the retinoblastoma tumor suppressor protein to induce cell cycle arrest (Xia et al., 2003), and mxi1 is one member of a network of proteins that opposes myc signaling to suppress proliferation (Grandori et al., 2000). After only 4 h of TCDD exposure, TCDD decreased expression of proliferating cell nuclear antigen (pcna), as well as two minichromosome maintenance genes, *mcm2* and *mcm5*, that play critical roles in DNA replication (Bailis and Forsburg, 2004). These are all known markers of proliferation (Saeed et al., 2003; Nolte et al., 2005). It is noteworthy that these cardiac-specific transcriptional responses occurred before any observable toxic responses. In addition, a halt in cellular proliferation would not produce noticeable changes in total cell number for at least several hours. Therefore, the plateau in cardiomyocyte number at 24 h after exposure (96 hpf) could be the result of a transcriptional process initiated shortly after TCDD exposure.

Although AHR/ARNT is likely to play roles in the cell beyond that of transcriptional activation, our model suggests that TCDD initiates cardiotoxicity by transcriptional misregulation of genes in the developing heart. This is based on the well known ability of the AHR/ARNT heterodimer to act as a transcriptional regulator and the demonstration that deletion of the nuclear localization sequence from AHR in mice results in resistance to TCDD toxicity (Bunger et al., 2003). This model is reinforced by the rapid changes in transcript abundance observed in heart cells after TCDD exposure. In such a model, the transcriptional changes that lead to toxicity should be identifiable among the sets of transcripts that are altered shortly after TCDD exposure.

Acknowledgments

We thank Dorothy Nesbit for technical assistance with the real-time PCR analysis and Dagmara S. Antkiewicz for expertise with microscopy imaging. We also thank M. Waters and B. Guy for laboratory assistance.

References

Antkiewicz DS, Burns CG, Carney SA, Peterson RE, and Heideman W (2005) Heart malformation is an early response to TCDD in embryonic zebrafish. *Toxicol Sci* **84:**368–377.

Bailis JM and Forsburg SL (2004) MCM proteins: DNA damage, mutagenesis and repair. *Curr Opin Genet Dev* **14:**17–21.

Belair CD, Peterson RE, and Heideman W (2001) Disruption of erythropoiesis by dioxin in the zebrafish. *Dev Dyn* **222:**581–594.

Brunstrom B and Lund J (1988) Differences between chick and turkey embryos in sensitivity to 3,3′,4,4′-tetrachloro-biphenyl and in concentration/affinity of the hepatic receptor for 2,3,7,8-tetrachlorodibenzo-*p*-dioxin. *Comp Biochem Physiol C* **91:**507–512.

Bunger MK, Moran SM, Glover E, Thomae TL, Lahvis GP, Lin BC, and Bradfield CA (2003) Resistance to 2,3,7,8-tetrachlorodibenzo-*p*-dioxin toxicity and abnormal liver development in mice carrying a mutation in the nuclear localization sequence of the aryl hydrocarbon receptor. *J Biol Chem* **278:**17767–17774.

Burns CG and MacRae CA (2006) Purification of hearts from zebrafish embryos [published erratum appears in *Biotechniques* **40:**596, 2006]. *Biotechniques* **40:**274, 276, 278.

Canga L, Levi R, and Rifkind AB (1988) Heart as a target organ in 2,3,7,8-tetrachlorodibenzo-*p*-dioxin toxicity: decreased beta-adrenergic responsiveness and evidence of increased intracellular calcium. *Proc Natl Acad Sci USA* **85:**905–909.

Canga L, Paroli L, Blanck TJ, Silver RB, and Rifkind AB (1993) 2,3,7,8-Tetrachlorodibenzo-*p*-dioxin increases cardiac myocyte intracellular calcium and progressively impairs ventricular contractile responses to isoproterenol and to calcium in chick embryo hearts. *Mol Pharmacol* **44:**1142–1151.

Carney SA, Peterson RE, and Heideman W (2004) 2,3,7,8-Tetrachlorodibenzo-*p*-dioxin activation of the aryl hydrocarbon receptor/aryl hydrocarbon receptor nuclear translocator pathway causes developmental toxicity through a CYP1A-independent mechanism in zebrafish. *Mol Pharmacol* **66:**512–521.

Chambers DJ (2003) Mechanisms and alternative methods of achieving cardiac arrest. *Ann Thorac Surg* **75:**S661–S666.

Cheung MO, Gilbert EF, and Peterson RE (1981) Cardiovascular teratogenicity of 2,3,7,8-tetrachlorodibenzo-*p*-dioxin in the chick embryo. *Toxicol Appl Pharmacol* **61:**197–204.

Coucelo J, Joachim N, and Coucelo J (2000) Calculation of volumes and systolic

indices of heart ventricle from *Halobatrachus didactylus*: echocardiographic noninvasive method. *J Exp Zool* **286:**585–595.
Dong W, Teraoka H, Tsujimoto Y, Stegeman JJ, and Hiraga T (2004) Role of aryl hydrocarbon receptor in mesencephalic circulation failure and apoptosis in zebrafish embryos exposed to 2,3,7,8-tetrachlorodibenzo-*p*-dioxin. *Toxicol Sci* **77:** 109–116.
Dong W, Teraoka H, Yamazaki K, Tsukiyama S, Imani S, Imagawa T, Stegeman JJ, Peterson RE, and Hiraga T (2002) 2,3,7,8-Tetrachlorodibenzo-*p*-dioxin toxicity in the zebrafish embryo: local circulation failure in the dorsal midbrain is associated with increased apoptosis. *Toxicol Sci* **69:**191–201.
Ebert AM, Hume GL, Warren KS, Cook NP, Burns CG, Mohideen MA, Siegal G, Yelon D, Fishman MC, and Garrity DM (2005) Calcium extrusion is critical for cardiac morphogenesis and rhythm in embryonic zebrafish hearts. *Proc Natl Acad Sci USA* **102:**17705–17710.
Eisen MB, Spellman PT, Brown PO, and Botstein D (1998) Cluster analysis and display of genome-wide expression patterns. *Proc Natl Acad Sci USA* **95:**14863–14868.
Elonen GE, Sphear RL, Holcombe GW, and Johnson RD (1998) Comparative toxicity of 2,3,7,8-tetrachlorodibenzo-*p*-dioxin to seven freshwater species during early life-stage development. *Environ Toxicol Chem* **17:**472–483.
Fernandez-Salguero PM, Hilbert DM, Rudikoff S, Ward JM, and Gonzalez FJ (1996) Aryl-hydrocarbon receptor-deficient mice are resistant to 2,3,7,8-tetrachlorodibenzo-*p*-dioxin-induced toxicity. *Toxicol Appl Pharmacol* **140:**173–179.
Fernandez-Salguero PM, Ward JM, Sundberg JP, and Gonzalez FJ (1997) Lesions of aryl-hydrocarbon receptor-deficient mice. *Vet Pathol* **34:**605–614.
Fisher MT, Nagarkatti M, and Nagarkatti PS (2004) Combined screening of thymocytes using apoptosis-specific cDNA array and promoter analysis yields novel gene targets mediating TCDD-induced toxicity. *Toxicol Sci* **78:**116–124.
Frueh FW, Hayashibara KC, Brown PO, and Whitlock JP Jr (2001) Use of cDNA microarrays to analyze dioxin-induced changes in human liver gene expression. *Toxicol Lett* **122:**189–203.
Grandori C, Cowley SM, James LP, and Eisenman RN (2000) The Myc/Max/Mad network and the transcriptional control of cell behavior. *Annu Rev Cell Dev Biol* **16:**653–699.
Guiney PD, Walker MK, Spitsbergen JM, and Peterson RE (2000) Hemodynamic dysfunction and cytochrome P4501A mRNA expression induced by 2,3,7,8-tetrachlorodibenzo-*p*-dioxin during embryonic stages of lake trout development. *Toxicol Appl Pharmacol* **168:**1–14.
Hahn ME (2003) Evolutionary and physiological perspectives on Ah receptor function and dioxin toxicity, in *Dioxins and Health* (Schecter A GT ed) pp 559–602, John Wiley and Sons, Hoboken, NJ.
Handley-Goldstone HM, Grow MW, and Stegeman JJ (2005) Cardiovascular gene expression profiles of dioxin exposure in zebrafish embryos. *Toxicol Sci* **85:**683–693.
Hanlon PR, Zheng W, Ko AY, and Jefcoate CR (2005) Identification of novel TCDD-regulated genes by microarray analysis. *Toxicol Appl Pharmacol* **202:**215–228.
Helder T (1980) Effects of 2,3,7,8-tetrachlorodibenzo-*p*-dioxin (TCDD) on early life stages of the pike (*Esox lucius*, *L.*). *Sci Total Environ* **14:**183–193.
Helder T (1981) Effects of 2,3,7,8-tetrachlorodibenzo-dioxin (TCDD) on early life stages of rainbow trout (*Salmo gairdneri*, *Richardson*). *Toxicology* **19:**101–112.
Henry TR, Spitsbergen JM, Hornung MW, Abnet CC, and Peterson RE (1997) Early life stage toxicity of 2,3,7,8-tetrachlorodibenzo-*p*-dioxin in zebrafish (*Danio rerio*). *Toxicol Appl Pharmacol* **142:**56–68.
Hornung MW, Spitsbergen JM, and Peterson RE (1999) 2,3,7,8-Tetrachlorodibenzo-*p*-dioxin alters cardiovascular and craniofacial development and function in sac fry of rainbow trout (*Oncorhynchus mykiss*). *Toxicol Sci* **47:**40–51.
Hove JR, Koster RW, Forouhar AS, Acevedo-Bolton G, Fraser SE, and Gharib M (2003) Intracardiac fluid forces are an essential epigenetic factor for embryonic cardiogenesis. *Nature (Lond)* **42:**172–177.
Hu N, Sedmera D, Yost HJ, and Clark EB (2000) Structure and function of the developing zebrafish heart. *Anat Rec* **260:**148–157.
Ivnitski I, Elmaoued R, and Walker MK (2001) 2,3,7,8-Tetrachlorodibenzo-*p*-dioxin (TCDD) inhibition of coronary development is preceded by a decrease in myocyte proliferation and an increase in cardiac apoptosis. *Teratol* **64:**201–212.
Jin B, Kim G, Park DW, and Ryu DY (2004) Microarray analysis of gene regulation in the Hepa1c1c7 cell line following exposure to the DNA methylation inhibitor 5-aza-2′-deoxycytidine and 2,3,7,8-tetrachlorodibenzo-*p*-dioxin. *Toxicol In Vitro* **18:**659–664.
Lahvis G, Lindell S, Thomas R, McCuskey R, Murphy C, Glover E, Bentz M, Southard J, and Bradfield C (2000) Portosystemic shunting and persistent fetal vascular structures in aryl hydrocarbon receptor-deficient mice. *Proc Natl Acad Sci USA* **97:**10442–10447.
Lin TM, Ko K, Moore RW, Buchanan DL, Cooke PS, and Peterson RE (2001) Role of the aryl hydrocarbon receptor in the development of control and 2,3,7,8-tetrachlorodibenzo-*p*-dioxin-exposed male mice. *J Toxicol Environ Health* **64:**327–342.
Lund AK, Goens MB, Kanagy NL, and Walker MK (2003) Cardiac hypertrophy in aryl hydrocarbon receptor null mice is correlated with elevated angiotensin II, endothelin-1, and mean arterial blood pressure. *Toxicol Appl Pharmacol* **193:**177–187.
Mably JD, Mohideen MA, Burns CG, Chen JN, and Fishman MC (2003) heart of glass regulates the concentric growth of the heart in zebrafish. *Curr Biol* **13:**2138–2147.
Martinez JM, Afshari CA, Bushel PR, Masuda A, Takahashi T, and Walker NJ (2002) Differential toxicogenomic responses to 2,3,7,8-tetrachlorodibenzo-*p*-dioxin in malignant and nonmalignant human airway epithelial cells. *Toxicol Sci* **69:** 409–423.
Nolte T, Kaufmann W, Schorsch F, Soames T, and Weber E (2005) Standardized assessment of cell proliferation: the approach of the RITA-CEPA working group. *Exp Toxicol Pathol* **57:**91–103.
Prasch AL, Teraoka H, Carney SA, Dong W, Hiraga T, Stegeman JJ, Heideman W, and Peterson RE (2003) Aryl hydrocarbon receptor 2 mediates 2,3,7,8-tetrachlorodibenzo-*p*-dioxin developmental toxicity in zebrafish. *Toxicol Sci* **76:** 138–150.
Puga A, Barnes SJ, Dalton TP, Chang C, Knudsen ES, and Maier MA (2000a) Aromatic hydrocarbon receptor interaction with the retinoblastoma protein potentiates repression of E2F-dependent transcription and cell cycle arrest. *J Biol Chem* **275:**2943–2950.
Puga A, Maier A, and Medvedovic M (2000b) The transcriptional signature of dioxin in human hepatoma HepG2 cells. *Biochem Pharmacol* **60:**1129–1142.
Rifkind AB, Sassa S, Reyes J, and Muschick H (1985) Polychlorinated aromatic hydrocarbon lethality, mixed-function oxidase induction, and uroporphyrinogen decarboxylase inhibition in the chick embryo: dissociation of dose-response relationships. *Toxicol Appl Pharmacol* **78:**268–279.
Rowlands JC and Gustafsson JA (1997) Aryl hydrocarbon receptor-mediated signal transduction. *Crit Rev Toxicol* **27:**109–134.
Saeed AI, Sharov V, White J, Li J, Liang W, Bhagabati N, Braisted J, Klapa M, Currier T, Thiagarajan M, et al. (2003) TM4: a free, open-source system for microarray data management and analysis. *Biotechniques* **34:**374–378.
Schiller NB, Shah PM, Crawford M, DeMaria A, Devereux R, Feigenbaum H, Gutgesell H, Reichek N, Sahn D, Schnittger I, et al. (1989) Recommendations for quantitation of the left ventricle by two-dimensional echocardiography. American Society of Echocardiography Committee on Standards, Subcommittee on Quantitation of Two-Dimensional Echocardiograms. *J Am Soc Echocardiogr* **2:**358–367.
Schmidt JV and Bradfield CA (1996) Ah receptor signaling pathways. *Annu Rev Cell Dev Biol* **12:**55–89.
Schmidt JV, Su GH, Reddy JK, Simon MC, and Bradfield CA (1996) Characterization of a murine Ahr null allele: involvement of the Ah receptor in hepatic growth and development. *Proc Natl Acad Sci USA* **93:**6731–6736.
Sommer RJ, Hume AJ, Ciak JM, Vannostrand JJ, Friggens M, and Walker MK (2005) Early developmental 2,3,7,8-tetrachlorodibenzo-*p*-dioxin exposure decreases chick embryo heart chronotropic response to isoproterenol but not to agents affecting signals downstream of the beta-adrenergic receptor. *Toxicol Sci* **83:**363–371.
Spitsbergen JM, Walker MK, Olson JR, and Peterson RE (1991) Pathologic alterations in early life stages of lake trout, *Salvelinus namaycush*, exposed to 2,3,7,8-tetrachlorodibenzo-*p*-dioxin as fertilized eggs. *Aquat Toxicol* **19:**41–72.
Teraoka H, Dong W, Ogawa S, Tsukiyama S, Okuhara Y, Niiyama M, Ueno N, Peterson RE, and Hiraga T (2002) 2,3,7,8-Tetrachlorodibenzo-*p*-dioxin toxicity in the zebrafish embryo: altered regional blood flow and impaired lower jaw development. *Toxicol Sci* **65:**192–199.
Thackaberry EA, Bedrick EJ, Goens MB, Danielson L, Lund AK, Gabaldon D, Smith SM, and Walker MK (2003) Insulin regulation in AhR-null mice: embryonic cardiac enlargement, neonatal macrosomia, and altered insulin regulation and response in pregnant and aging AhR-null females. *Toxicol Sci* **76:**407–417.
Thackaberry EA, Gabaldon DM, Walker MK, and Smith SM (2002) Aryl hydrocarbon receptor null mice develop cardiac hypertrophy and increased hypoxia-inducible factor-1alpha in the absence of cardiac hypoxia. *Cardiovasc Toxicol* **2:**263–274.
Thackaberry EA, Jiang Z, Johnson CD, Ramos KS, and Walker MK (2005a) Toxicogenomic profile of 2,3,7,8-tetrachlorodibenzo-*p*-dioxin in the murine fetal heart: modulation of cell cycle and extracellular matrix genes. *Toxicol Sci* **88:**231–241.
Thackaberry EA, Nunez BA, Ivnitski-Steele ID, Friggins M, and Walker MK (2005b) Effect of 2,3,7,8-tetrachlorodibenzo-*p*-dioxin on murine heart development: alteration in fetal and postnatal cardiac growth, and postnatal cardiac chronotropy. *Toxicol Sci* **88:**242–249.
Vezina CM, Walker NJ, and Olson JR (2004) Subchronic exposure to TCDD, PeCDF, PCB126, and PCB153: effect on hepatic gene expression. *Environ Health Perspect* **112:**1636–1644.
Walisser JA, Bunger MK, Glover E, and Bradfield CA (2004) Gestational exposure of Ahr and Arnt hypomorphs to dioxin rescues vascular development. *Proc Natl Acad Sci USA* **101:**16677–16682.
Walker MK and Catron TF (2000) Characterization of cardiotoxicity induced by 2,3,7,8-tetrachlorodibenzo-*p*-dioxin and related chemicals during early chick embryo development. *Toxicol Appl Pharmacol* **167:**210–221.
Walker MK, Pollenz RS, and Smith SM (1997) Expression of the aryl hydrocarbon receptor (AhR) and AhR nuclear translocator during chick cardiogenesis is consistent with 2,3,7,8-tetrachlorodibenzo-*p*-dioxin-induced heart defects. *Toxicol Appl Pharmacol* **143:**407–419.
Wisk JD and Cooper KR (1990) The stage specific toxicity of 2,3,7,8-tetrachlorodibenzo-*p*-dioxin in embryos of the Japanese medaka (*Oryzias latipes*). *Environ Toxicol Chem* **9:**1159–1169.
Xia X, Cheng A, Akinmade D, and Hamburger AW (2003) The N-terminal 24 amino acids of the p55 gamma regulatory subunit of phosphoinositide 3-kinase binds Rb and induces cell cycle arrest. *Mol Cell Biol* **23:**1717–1725.

Address correspondence to: Warren Heideman, University of Wisconsin-Madison, School of Pharmacy, 5111 Rennebohm Hall, 777 Highland Avenue, Madison, WI 53705. E-mail: wheidema@wisc.edu